

USGS Award: G09AP00078

TITLE: RAPID AND ROBUST SEISMIC MOMENTS FROM VARIABLE-PERIOD SURFACE WAVE MAGNITUDES

PRINCIPAL INVESTIAGATOR:

Jessie Bonner
Weston Geophysical Corp.
107 E. Lufkin Ave. Suite 450
Lufkin, TX, 75904
936-238-9690 (no fax)
bonner@westongeophysical.com

PERIOD OF PERFORMANCE: June 2009-June 2010

ADDITIONAL CONTRIBUTORS:

Robert Herrmann (St. Louis University), Harley Benz (USGS NEIC)

ABSTRACT

We demonstrate that surface wave magnitudes (M_s), measured at local, regional, and teleseismic distances, can be used as a rapid and robust estimator of seismic moment magnitude (M_w). We used the Russell (2006) variable-period surface wave magnitude formula, henceforth called $M_s(\text{VMAX})$, to estimate the M_s for 165 North American events with $3.2 < M_w < 6.5$ at distances ranging from 48 to 5268 km. Of the 7370 event-station pairs, more than half (4051) of the measurements were at distances less than 1000 km. M_w estimated from broadband waveform modeling (Herrmann et al., 2008) were regressed against $M_s(\text{VMAX})$. M_w can be estimated from $M_s(\text{VMAX})$ using the relationship: $M_w = 1.91 + 0.66 * M_s(\text{VMAX})$ for $2 < M_s < 6$. We find similar results for earthquakes in the Korean Peninsula and central Italy. The observed scatter of the $M_w[M_s(\text{VMAX})]$ with respect to $M_w[\text{Waveform Modeling}]$ was approximately ± 0.2 magnitude units (m.u). The residuals between $M_w[M_s(\text{VMAX})]$ and $M_w[\text{Waveform Modeling}]$ show a significant focal mechanism effect, especially when strike-slip events are compared to other mechanisms. Validation testing of this method suggests that $M_s(\text{VMAX})$ -predicted M_w 's can be estimated within minutes after the origin of an event and are typically within ± 0.2 m.u. of the final $M_w[\text{Waveform Modeling}]$. While M_w estimated from $M_s(\text{VMAX})$ has a slightly higher variance than waveform modeling results, it can be measured on the first short-period surface wave observed at a local or near-regional distance seismic station after a preliminary epicentral location has been formed. Therefore, it may be used to make rapid measurements of M_w which are needed by Government agencies for early warning systems.

TABLE OF CONTENTS

ABSTRACT	1
TABLE OF CONTENTS	2
TABLE OF FIGURES	2
TABLE OF TABLES	3
INTRODUCTION	4
M_s (VMAX) VERSUS M_w RELATIONSHIP FOR NORTH AMERICA	7
VALIDATION TESTING	17
CONCLUSIONS	20
DATA AND RESOURCES	21
ACKNOWLEDGEMENTS	21
REFERENCES	21
BIBLIOGRAPHY	23
APPENDIX: APPLICATION IN CENTRAL ITALY	24

TABLE OF FIGURES

Figure 1. Examples of the M_s (VMAX) methodology. a). Filter combs of Rayleigh waves at periods of 8,10,12,...,24 seconds for a Montana earthquake recorded at DUG. The first vertical line is 4.0 km/sec while the last line is 2.0 km/sec. The middle line marks the largest amplitude. Amplitudes are in nm. b). Network results. The solid lines represent signal-based magnitudes with the period of maximum amplitude for each station shown as the small circles. The thick line is the variable-period magnitudes for station DUG. The dashed lines are background noise levels. The station magnitudes were averaged to form a network M_s (VMAX) of 4.42 for this event. An M_w of 4.83 was determined for this event by Herrmann et al. (2008).	6
Figure 2. Earthquakes used in a study to determine the relationship between M_s (VMAX) and M_w in North America. Also shown are the focal mechanisms.	7
Figure 3. Orthogonal linear regressions of a) scalar moment ($\log M_0$) and b) moment magnitude (M_w) versus M_s (VMAX). The moments were determined from broadband waveform modeling (Herrmann <i>et al.</i> , 2008). The solid lines are described by the linear equations at the top of each plot.	13
Figure 4. A comparison of the different linear regression methods described in Castellaro and Bormann (2007) applied to our M_s (VMAX) and moment data.	14
Figure 5. Scatter in $M_w[M_s$ (VMAX)] estimates as function of evaluation period and distance. The dashed line represents ± 0.2 m.u. while ± 1 standard deviation (σ) is shown as the solid lines (for most periods, the two are very similar).	15
Figure 6. The dependence $M_w[M_s$ (VMAX)] as a function of focal mechanism and depth. The mechanisms are based on the Zoback (1992) classification scheme and focal mechanisms of Herrmann et al. (2008). The faulting definitions include: SS=Strike-Slip, TF=Thrust Fault,	

NF=Normal Fault, TS=Thrust with Strike-Slip component, NS=Normal with Strike-Slip component and XX=Unknown. The residuals between M_w [Waveform Modeling] and M_w [M_s (VMAX)] have a definable faulting mechanism effect, especially when strike-slip events are compared to those with other mechanisms..... 16

Figure 7. M_w [M_s (VMAX)] as a function of time after event origin for three events in our validation dataset. The events occurred on a) 24 March 2009 at 11:55:43 b) 03 July 2009 at 11:00:19 and c) 29 July 2009 at 10:00:36. The mean for each station is shown as a circle with ± 1 standard deviation (σ) presented as the vertical error bars. The dashed horizontal line is the observed M_w based on waveform modeling..... 19

Figure 8. M_w [M_s (VMAX)] at five (5) minutes after event origin versus M_w [Waveform Modeling]. The solid line is the 1:1 relation with ± 0.2 m.u. plotted as dashed lines. Vertical error bars represent $\pm 1 \sigma$ 20

TABLE OF TABLES

Table 1. Origin Information for 165 Events Used to Derive an M_w : M_s (VMAX) Relationship ...	9
Table 2. Comparison of Different Regression Methods to Convert M_s (MVAX) to Moments....	14
Table 3. Statistical Analysis of M_w [Waveform Modeling] - M_w [M_s (VMAX)]	17
Table 4. Origin Information for the Validation Test	18

INTRODUCTION

The Prompt Assessment of Global Earthquakes for Response (PAGER) system is a critical service of the United States Geological Survey National Earthquake Information Center (USGS NEIC). Rapid estimates of moment magnitude (M_w) are needed in PAGER (Earle *et al.*, 2008) to help predict the damage and casualties from strong earthquakes. The predictions are, in turn, provided to authorities responsible for societal response to earthquakes.

This paper examines the automatic estimation of M_w for continental earthquakes by the computation of local-to-regional surface-wave magnitudes (M_s) and subsequent conversion to M_w . The benefit of this approach is that an initial estimate of M_w , with perhaps a slightly higher variance than waveform modeling methods, can be completed as soon as the short and intermediate-period (8-25 second) surface waves have been observed, without having to wait for the detailed waveform-based moment tensor inversion. This means that an estimate of M_w can be made from near-regional data (< 10 degrees) even before the estimation of a moment tensor based on the long-period teleseismic P -wave can begin and long before the inversion of a Centroid Moment Tensor (CMT) from surface-wave data can be initiated.

Surface Wave Magnitudes. Many surface wave magnitude scales have been developed during the past century (Gutenberg, 1945; Vaněk *et al.*, 1962; Marshall and Basham, 1972; Von Seggern, 1977; Herak and Herak, 1993; Rezapour and Pearce, 1998; Stevens and McLaughlin, 2001; Bormann *et al.*, 2009). Bormann *et al.* (2009) provide an excellent review of the development of several of these formulas and addresses confusion about their applications.

A considerable problem for surface wave magnitude estimation at local and regional distances on continental paths can result from the Airy phase. An Airy phase is caused by a local minimum in the group velocity curve, typically at periods less than 20 seconds, which often results in large amplitude surface waves that could bias M_s magnitudes. Russell (2006) sought to solve this problem by passing the surface waves, including the Airy phase, through a series of zero-phase Butterworth filters. This new method can effectively measure surface-wave magnitudes at local, regional and teleseismic distances, at variable periods between 8 and 25 seconds. The magnitude equation is:

$$M_{s(b)} = \log(a_b) + \frac{1}{2} \log(\sin(\Delta)) + 0.0031 \left(\frac{20}{T} \right)^{1.8} \Delta - 0.66 \log \left(\frac{20}{T} \right) - \log(f_c) - 0.43, \quad (1)$$

where a_b is the amplitude of the Butterworth-filtered surface waves (zero-to-peak in nanometers) and f_c is the filter frequency of a causal band-pass filter implemented as a cascade of low-pass and high-pass Butterworth filters with corner frequencies of $1/T - f_c$, $1/T + f_c$, respectively. At the reference period $T=20$ seconds, the equation is equivalent to Von Seggern's formula (1977) scaled to Vaněk *et al.* (1962) at $\Delta=50$ degrees. For periods $8 \leq T \leq 25$, the equation is corrected to $T=20$ seconds, accounting for frequency-dependent source effects, attenuation, and dispersion.

M_s (VMAX) Methodology. Bonner *et al.*, (2006) developed the M_s (VMAX) measurement technique, which refers to Variable-period MAXimum amplitude surface waves, based on

Equation 1. They applied a series of zero-phase 3rd-order Butterworth filters to the data with the corner frequencies $(1/T)-f_c$, $(1/T)+f_c$, where

$$f_c \leq \frac{G_{\min}}{T\sqrt{\Delta}} . \quad (2)$$

For continental paths between 8 and 25 seconds, G_{\min} , which is based on dispersion effects, is set to 0.6. The center periods are placed at 1-second intervals between 8 and 25 seconds. Bonner et al., (2006) construct the envelope function of the filtered signal and measure the maximum zero-to-peak vertical-component amplitude in a group velocity window between 2.0 and 4.0 km/sec. The procedure is automated based on signal-to-noise requirements within the analysis window. In Figure 1a, we show examples of filter panels from an $M_w=4.83$ Montana earthquake recorded at station DUG at a near-regional distance of 509 km. Note the differences in the Rayleigh-wave amplitudes between 20-secs period, where the standard NEIC M_s is measured, and 8-14 secs period.

After filtering, the next stage in the $M_s(\text{VMAX})$ methodology for a given station is to record the maximum amplitude in each of the 18 filter bands and then use Equation 1 to calculate a variable-period surface-wave magnitude. As a result, 18 different magnitudes are estimated for each station recording the event (Figure 1b). The variable-period filtered data (Figure 1b) is then searched to determine the period of the maximum Butterworth filter-corrected amplitude, and the magnitude calculated at that period is used as the final estimate for that station. As an example, the period of maximum corrected amplitude for the DUG recording occurred at $T=10$ seconds. For this Montana event, all of the $M_s(\text{VMAX})$ estimates were made at periods less than 18 seconds. The same processing is conducted for all stations that recorded the event allowing for estimation of a network-averaged $M_s(\text{VMAX})$ (4.42), an interstation standard deviation (0.13), and surface-wave magnitude “noise floors” at each station (see Figure 1b dashed lines). To simplify this method operationally, one does not have to calculate 18 different magnitudes for each station and could instead initially search for the period of maximum amplitude and estimate a single $M_s(\text{VMAX})$. Bonner et al. (2006) prefer the multiple-magnitude approach to better understand path and focal mechanism effects on $M_s(\text{VMAX})$.

Bonner et al. (2006) have shown that $M_s(\text{VMAX})$ estimates measured at epicentral distances as close as 50 km do not differ significantly from estimates made at teleseismic distances. They note less than -0.002 magnitude units per degree distance dependence on $M_s(\text{VMAX})$, which has similarly been noted for the broadband $M_s(\text{BB})$ proposed by Bormann et al. (2009). This small distance dependence and the ability to measure $M_s(\text{VMAX})$ at local and regional distances, even with complications associated with Airy phases, led us to ponder whether $M_s(\text{VMAX})$ estimates could be used as a rapid and robust estimator of seismic moment. In this paper, we use the $M_s(\text{VMAX})$ methodology to estimate M_s at local, regional, and teleseismic distances using a North American dataset. We then present the relationship between $M_s(\text{VMAX})$ and M_w for this dataset and discuss the effects of focal mechanism on the scatter. Finally, we apply the new relationship to local and near-regional data to estimate moments within a few minutes (e.g., 5 minutes) after the origin of North American seismic events.

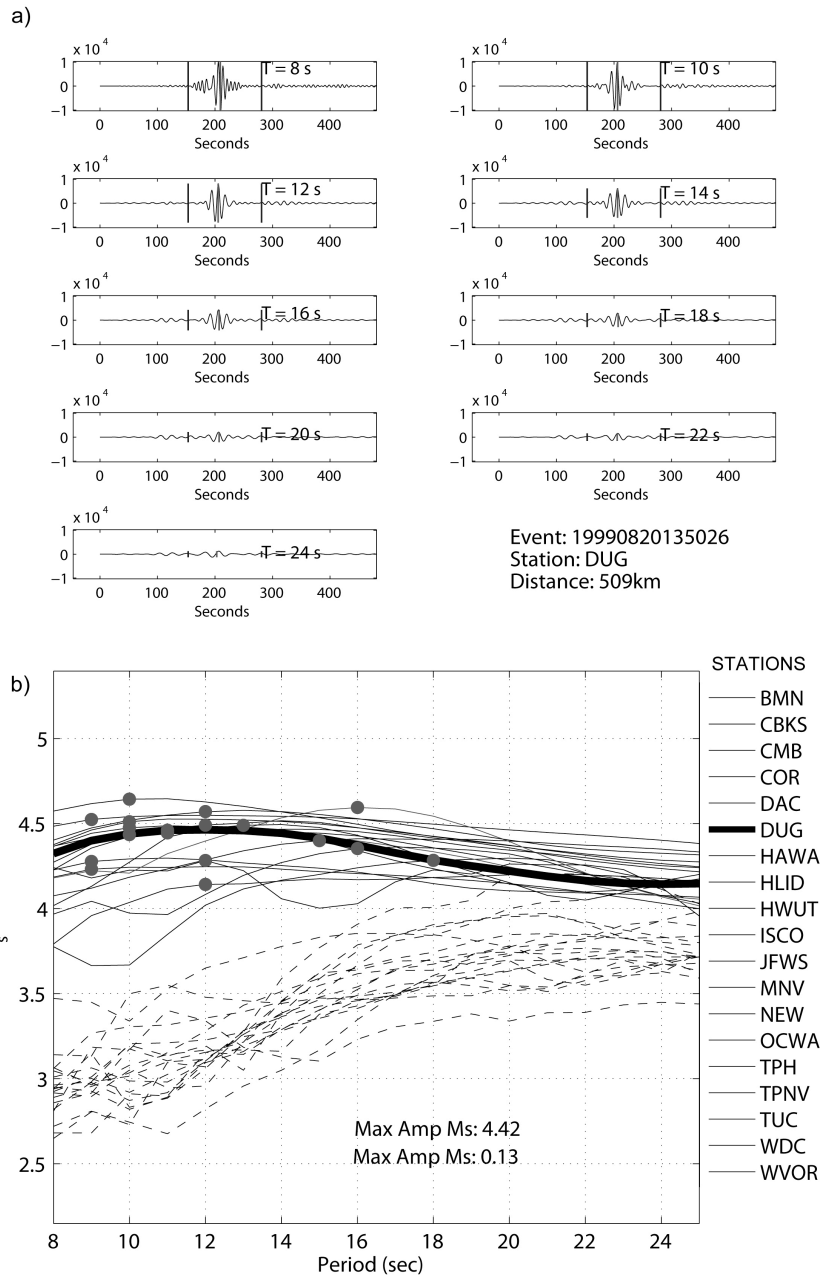


Figure 1. Examples of the $M_s(\text{VMAX})$ methodology. a). Filter combs of Rayleigh waves at periods of 8,10,12,...,24 seconds for a Montana earthquake recorded at DUG. The first vertical line is 4.0 km/sec while the last line is 2.0 km/sec. The middle line marks the largest amplitude. Amplitudes are in nm. b). Network results. The solid lines represent signal-based magnitudes with the period of maximum amplitude for each station shown as the small circles. The thick line is the variable-period magnitudes for station DUG. The dashed lines are background noise levels. The station magnitudes were averaged to form a network $M_s(\text{VMAX})$ of 4.42 for this event. An M_w of 4.83 was determined for this event by Herrmann et al. (2008).

M_s (VMAX) VERSUS M_w RELATIONSHIP FOR NORTH AMERICA

Data. We have used the M_s (VMAX) method to estimate surface-wave magnitudes for 165 events in North America (Table 1). The events were part of a database of crustal-depth (< 30 km) North American events for which Herrmann *et al.* (2008) determined an M_w using broadband waveform modeling. The waveform modeling for these events can be found at http://www.eas.slu.edu/Earthquake_Center/MECH.NA/ (last accessed March, 2010). The events were $3.2 < M_w < 6.5$, occurred between 1995 and 2008, and include events with predominantly continental paths. Normal, reverse, and strike-slip mechanisms are represented. Figure 2 shows the geographic distribution of these events and the focal mechanisms. Data from these events were downloaded from the Incorporated Research Institutions in Seismology (IRIS) and the USGS (see Data Resources section for further details), corrected for their instrument response, and converted to displacement in nanometers. M_s (VMAX) was estimated for stations at distances ranging from 48 to 5268 km. Of the 7370 event-station pairs, 4051 of the measurements were at distances < 1000 km. The 1000 km distance range is very important for our proposed rapid estimation of M_w from the M_s estimates.

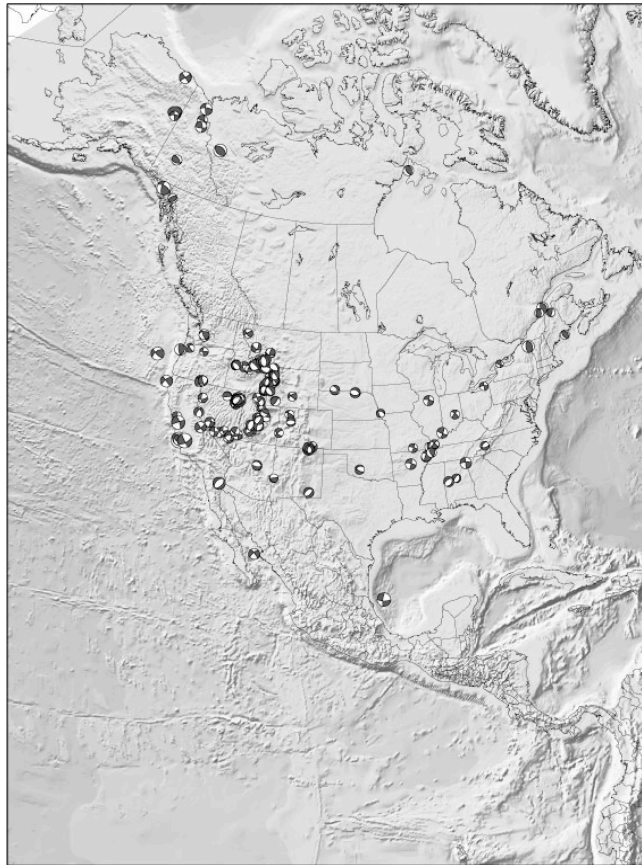


Figure 2. Earthquakes used in a study to determine the relationship between M_s (VMAX) and M_w in North America. Also shown are the focal mechanisms.

Results. We have derived a relationship between the scalar seismic moment ($\log M_o$) and $M_s(\text{VMAX})$ using the North American earthquakes. Broadband waveform modeling (Herrmann et al., 2008) was used to estimate $\log M_o$ which was then orthogonally regressed (e.g., Castellaro and Bormann, 2007) against $M_s(\text{VMAX})$ (Figure 3). We have determined that $\log M_o$ can be estimated from surface wave magnitudes using the relationship:

$$\log M_o = 18.9 + 0.99 M_s(\text{VMAX}) \quad (3)$$

for the events in our database with $2 < M_s < 6$. Three events in our database were outside this magnitude range and were not considered in the regression analysis. Equation 3 is very similar to a global study conducted by Ekström and Dziewonski (1988) who observed that:

$$\log M_o = 19.24 + M_s \quad (4)$$

for $M_s < 5.3$.

Castellaro and Bormann (2007) provide an informative discussion on the types of regressions for converting magnitude from one type to another. These include the standard least-squares regression (SR), inverted standard least squares regression (ISR), general orthogonal regression (GOR), and particular orthogonal regression (OR). The OR method is best used when the true error for one or both of the magnitudes is unknown. In our case, we compute measurement errors for the $M_s(\text{VMAX})$ (see Table 2); however the variance for the moment estimates from broadband waveform modeling is difficult to compute due to dependence on station distribution, choice of velocity model, and other factors. For the OR method, the ratio of the variances between $\log M_o$ and $M_s(\text{VMAX})$ (a parameter Castellaro and Bormann define as η) is forced to be 1. Table 2 and Figure 4 provide a comparison of the slopes and intercepts for various regression methods and/or different values of η used to convert the $M_s(\text{VMAX})$ to moments. The formulas used in this manuscript to convert $M_s(\text{VMAX})$ to moment (e.g., Equation 4 and the upcoming Equation 6) are based on the OR method.

When the scalar $\log M_o$ is converted to moment magnitude (M_w) using the standard equation (Hanks and Kanamori, 1979):

$$M_w = \frac{2}{3} \log M_o - 10.7, \quad (5)$$

the OR relationship between M_w and $M_s(\text{VMAX})$ can be described by

$$M_w = 1.91 + 0.66 M_s(\text{VMAX}) \quad (6)$$

for $2 < M_s < 6$.

Table 1. Origin Information for 165 Events Used to Derive an M_w : M_s (VMAX) Relationship

Year	Month	Day	UTC	Latitude	Longitude	Depth (km)	M_w	Strike	Dip	Rake	M_s (VMAX)	STD
1995	1	28	6:26:21	44.51	-114.83	13	4.23	155	70	-30	3.46	0.08
1996	11	29	5:41:32	35.97	-90	11	3.78	120	65	-15	2.75	0.05
1997	5	16	1:23:20	40.58	-114.99	11	3.99	30	50	-100	3.15	0.09
1998	1	2	7:28:29	38.18	-112.46	16	4.52	235	50	20	3.92	0.07
1998	4	28	14:13:01	34.94	-98.51	19	3.88	120	70	-60	3.3	0.05
1998	6	20	21:16:20	43.26	-110.59	9	4.15	15	80	-55	3.58	0.07
1998	8	23	18:16:16	43.83	-111.03	14	3.85	205	55	10	3.16	0.07
1998	12	12	1:41:32	37.46	-116.29	11	4.24	350	60	-160	3.48	0.09
1998	12	22	1:17:46	48	-115.2	12	3.85	230	80	25	2.81	0.02
1999	6	30	15:27:32	40.64	-111.58	15	3.55	155	50	-85	2.56	0.03
1999	8	20	13:50:26	44.78	-112.77	14	4.83	260	40	-140	4.46	0.05
1999	9	9	11:38:43	38.89	-111.99	12	3.87	215	65	-75	3.09	0.07
1999	10	22	17:51:15	38.08	-112.73	6	4	180	40	-140	3.3	0.09
1999	12	22	8:03:31	38.76	-111.59	4	3.97	185	65	-95	3.15	0.11
2000	1	30	14:46:53	41.52	-109.81	7	4.1	30	75	80	3.43	0.07
2000	3	7	2:16:04	39.75	-110.83	13	3.99	150	20	-35	3.26	0.14
2000	4	8	11:30:21	46.39	-111.44	11	3.85	200	70	35	2.84	0.04
2000	5	24	4:22:06	46.35	-111.39	11	3.99	200	55	35	3.06	0.08
2000	5	26	21:58:46	42.18	-107.56	12	3.84	225	60	10	2.96	0.04
2000	5	27	21:58:18	38.33	-108.86	13	3.77	125	60	-15	2.95	0.06
2000	6	28	14:28:30	46.69	-113.58	12	4.13	115	70	-155	3.26	0.08
2000	9	1	19:02:59	37.7	-115.85	9	3.62	70	85	-20	2.51	0.09
2000	10	12	9:32:33	40.53	-119.51	8	3.82	70	60	-35	3.09	0.17
2000	11	10	19:14:05	46.4	-111.38	13	3.79	190	80	50	2.82	0.17
2000	11	19	12:54:30	40.49	-119.51	11	3.93	65	65	-25	3.15	0.05
2000	11	24	4:20:06	44.82	-110.59	6	4.46	110	65	-110	3.86	0.07
2001	2	23	21:43:50	38.73	-112.56	10	4.28	195	40	-85	3.3	0.09
2001	4	21	17:18:56	42.92	-111.39	10	5.1	349	47	-105	4.92	0.07
2001	5	4	6:42:12	35.19	-92.19	5	4.34	20	85	-165	3.62	0.05
2001	7	19	20:15:34	38.74	-111.55	2	4.23	190	65	-100	3.55	0.13
2001	9	4	12:45:53	37.15	-104.64	3	4.18	215	30	-80	3.5	0.07
2001	9	5	10:52:07	37.14	-104.47	2	4.44	190	25	-130	3.88	0.07
2002	1	29	4:36:58	43.58	-110.61	16	3.79	30	80	-15	2.5	0.01
2002	1	31	18:17:45	40.28	-107.7	11	3.87	290	70	40	2.97	0.11
2002	3	24	10:44:07	37.01	-115.1	11	4.06	180	65	-170	3.02	0.06

2002	3	31	18:35:01	43.16	-110.73	9	3.7	325	35	-135	2.73	0.18
2002	4	20	10:50:44	44.51	-73.66	10	4.97	360	35	80	4.62	0.11
2002	6	18	17:37:13	37.97	-87.78	19	4.5	120	80	10	3.66	0.07
2002	10	22	4:11:16	43.18	-110.83	11	4.33	355	55	-105	3.62	0.12
2002	11	3	20:41:56	42.81	-98.9	8	4.14	90	50	-110	3.32	0.08
2003	1	3	5:02:12	41.27	-111.82	13	3.87	170	60	-75	3.06	0.07
2003	4	17	1:04:19	39.55	-111.88	2	4.13	185	50	-85	3.7	0.1
2003	4	29	8:59:37	34.55	-85.5	12	4.59	275	75	5	3.76	0.05
2003	5	25	7:32:33	43.1	-101.75	15	3.93	85	60	-130	3.1	0.06
2003	5	29	22:52:14	38.26	-117.9	11	3.82	270	85	-15	2.78	0.04
2003	6	6	12:29:33	36.89	-88.99	5	4.02	165	85	15	3.21	0.09
2003	6	8	10:14:54	41.22	-116.36	11	3.79	75	80	85	3.09	0.07
2003	8	16	5:09:20	36.8	-91.72	5	3.71	25	80	-165	2.71	0.04
2003	8	21	7:56:54	44.09	-110.53	5	4.2	295	55	-100	3.6	0.1
2003	9	13	15:22:41	36.85	-104.99	4	4.05	170	55	-100	3.32	0.07
2003	11	15	20:11:59	38.22	-117.87	6	4.14	274	85	-10	3.02	0.06
2003	11	15	21:19:37	38.22	-117.87	10	4.07	264	70	-15	3.01	0.06
2003	11	23	12:19:59	40.73	-115.15	10	4.19	25	50	-90	3.38	0.06
2003	12	22	19:15:56	35.7	-121.1	7	6.54	115	35	80	6.75	0.08
2004	1	7	7:51:38	43.57	-110.38	5	4.8	145	55	-145	4.3	0.07
2004	1	7	8:44:21	43.57	-110.38	13	3.95	130	75	-155	2.93	0.07
2004	1	7	9:23:47	43.6	-110.35	15	3.89	220	75	25	2.75	0.08
2004	3	17	23:53:07	35.73	-121.07	5	4.62	105	55	70	3.96	0.09
2004	3	22	12:09:56	36.85	-104.85	4	4.39	175	55	-95	3.79	0.08
2004	4	7	15:54:12	43.61	-110.36	8	3.73	220	75	-5	2.56	0.1
2004	5	16	1:29:40	37.27	-114.96	6	3.97	350	75	-160	3.18	0.05
2004	6	15	8:34:21	36.73	-89.68	2	3.49	175	55	70	2.45	0.21
2004	6	22	8:55:28	32.53	-104.58	2	3.57	5	70	-110	2.51	0.07
2004	6	28	6:10:52	41.44	-88.96	7	4.15	20	90	-165	3.06	0.08
2004	6	30	12:21:45	42.17	-120.3	9	4.63	160	60	-120	4.03	0.11
2004	7	16	3:25:17	36.86	-89.16	5	3.46	140	70	20	2.21	0.12
2004	7	16	12:17:30	40.63	-95.56	12	3.53	290	55	-135	2.48	0.08
2004	8	1	6:50:46	36.89	-104.92	4	4.28	155	65	-120	3.6	0.07
2004	8	4	23:55:26	43.69	-78.25	3	3.19	125	65	35	2.04	0.05
2004	8	14	20:14:43	43.17	-111.02	8	3.63	20	75	-60	2.67	0.08
2004	8	16	21:05:54	46.68	-121.5	11	4.02	60	60	20	3.12	0.09
2004	8	19	6:06:03	44.66	-124.31	23	4.7	155	65	75	4.3	0.08
2004	8	19	23:51:49	33.18	-86.93	4	3.63	30	30	-100	2.57	0.1
2004	8	26	23:11:31	64.76	-86.28	23	4.24	155	60	80	3.7	0.05

2004	9	12	13:05:19	39.61	-85.75	13	3.83	320	75	15	2.58	0.15
2004	9	28	17:15:24	35.81	-120.37	8	5.89	140	85	-155	6.04	0.08
2004	10	1	19:22:18	37.4	-117.11	9	3.87	355	85	-155	2.77	0.08
2004	11	7	11:20:25	32.97	-87.9	3	4.25	35	40	-115	3.61	0.06
2004	11	16	18:21:28	42	-120.45	12	3.95	150	75	-130	3.2	0.08
2004	11	21	15:50:32	44.35	-114.01	13	3.86	195	60	55	2.89	0.14
2005	1	28	22:37:07	34.71	-111	4	3.76	135	75	-15	3.04	0.05
2005	1	30	11:37:50	34.76	-111.08	3	4	90	65	-100	3.33	0.09
2005	2	10	14:04:53	35.75	-90.23	14	4.11	55	80	-165	2.99	0.09
2005	3	6	6:17:49	47.75	-69.73	12	4.58	350	30	80	4.32	0.08
2005	5	1	12:37:32	35.83	-90.15	8	4.22	315	60	20	3.45	0.06
2005	6	2	11:35:10	36.14	-89.46	15	3.89	155	65	70	3.2	0.09
2005	6	11	11:16:10	42.27	-120.07	14	3.61	0	45	-45	2.58	0.1
2005	6	20	12:21:41	36.95	-88.96	4	3.6	320	80	15	2.17	0.1
2005	7	26	4:08:36	45.4	-112.55	10	5.47	115	55	-140	5.37	0.05
2005	7	26	7:12:46	45.43	-112.61	13	3.84	275	85	-130	3.13	0.09
2005	7	27	15:51:46	45.39	-112.62	12	3.99	360	55	-15	3.2	0.07
2005	7	28	2:29:30	45.5	-112.43	12	3.54	105	40	-130	2.5	0.08
2005	7	29	14:07:18	45.42	-112.6	11	3.52	170	40	-15	2.72	0.12
2005	8	7	5:28:34	45.5	-112.57	12	3.68	330	50	-50	2.75	0.05
2005	8	10	22:08:17	36.95	-104.86	4	4.88	160	40	-110	4.62	0.08
2005	8	12	20:53:48	42.2	-120.04	13	3.95	55	35	-10	2.96	0.09
2005	8	25	3:09:41	35.88	-82.8	8	3.65	90	60	-60	2.61	0.08
2005	9	16	15:09:44	39	-119.56	12	4.06	200	65	-50	3.39	0.08
2005	9	28	5:27:32	44.6	-116.07	11	3.84	170	65	20	3.08	0.07
2005	9	28	23:18:00	44.56	-115.99	8	3.64	160	50	0	2.5	0.02
2005	9	29	13:50:15	44.49	-116.06	9	3.85	355	75	55	2.82	0.13
2005	10	2	1:10:01	44.54	-115.99	7	3.84	150	30	-65	2.89	0.03
2005	10	31	0:23:30	44.9	-113.45	14	4.46	190	25	-25	3.74	0.09
2005	12	19	20:27:40	32.52	-104.57	5	4.14	230	40	-85	3.46	0
2006	1	11	10:02:36	43.55	-127.19	29	5.3	215	60	15	5.11	0.1
2006	1	18	9:47:45	45.42	-112.57	12	4.03	10	70	-25	3.17	0.08
2006	2	5	3:25:52	44.74	-111.88	13	4.43	135	35	-45	3.85	0.06
2006	2	10	21:48:13	39.55	-107.43	9	3.8	75	35	-100	2.7	0.11
2006	2	16	12:28:32	66.93	-135.83	11	4.12	85	90	30	3.18	0.1
2006	2	18	13:01:31	66.5	-142.11	13	4.17	70	85	-20	3.19	0.12
2006	3	5	10:42:16	64.93	-129.26	2	5.42	290	45	85	5.28	0.12
2006	3	29	3:36:54	66.41	-142.23	6	4.3	225	70	15	3.49	0.08
2006	4	7	8:31:40	47.38	-70.46	25	3.77	15	55	85	2.55	0.08

2006	5	18	10:16:21	44.17	-110.34	8	3.84	200	40	-30	3.06	0.05
2006	5	24	4:20:27	32.35	-115.19	12	5.09	215	45	-90	5.28	0.09
2006	6	7	4:04:03	43.35	-111.37	8	3.31	185	60	-90	1.54	0.23
2006	6	11	10:01:50	40.25	-111.07	14	3.5	235	25	35	2.7	0.04
2006	6	17	16:22:14	45.6	-111.91	10	3.83	175	50	-55	3.12	0.08
2006	6	18	0:05:33	45.6	-111.9	10	4.17	305	60	-120	3.41	0.07
2006	6	20	20:11:18	41.84	-81.17	4	3.55	275	75	0	2.17	0
2006	6	30	16:55:01	42.43	-111.5	10	4.15	10	65	-70	3.54	0.11
2006	7	14	9:34:46	47	-68.79	17	3.48	170	25	45	2.54	0.06
2006	7	14	17:06:01	42.43	-111.54	10	3.96	10	75	-70	3.42	0.09
2006	8	26	0:50:04	66.26	-142.49	21	4.48	230	75	-20	3.81	0.11
2006	8	27	2:58:23	66.27	-142.14	22	4.33	235	80	-15	3.56	0.13
2006	8	27	3:20:05	66.3	-142.25	20	4.35	225	75	-15	3.58	0.12
2006	9	1	23:44:49	66.43	-142.44	3	4.41	50	75	15	3.77	0.16
2006	9	2	19:54:59	42.43	-111.53	9	3.62	15	70	-65	2.54	0.2
2006	10	3	0:07:37	44.33	-68.17	2	3.87	340	35	85	3.24	0.09
2006	10	8	2:48:27	46.85	-121.6	12	4.31	255	40	25	3.7	0.07
2007	1	3	14:34:38	37.06	-104.9	2	4.38	205	50	-60	3.92	0.06
2007	1	9	15:49:35	59.37	-136.87	13	5.59	275	60	30	5.56	0.15
2007	1	24	11:30:15	37.41	-117.08	9	3.83	265	90	-10	2.79	0.04
2007	2	25	3:52:21	42.47	-110.67	11	3.96	325	70	-75	3.32	0.1
2007	2	28	11:47:41	41.06	-114.77	12	3.58	60	70	-25	2.64	0.03
2007	3	2	4:40:00	37.93	-122.14	12	4.3	80	80	10	3.4	0.06
2007	3	5	18:06:22	58.81	-134.44	1	3.81	35	35	85	3.25	0.08
2007	3	29	5:39:31	45.34	-112.58	11	3.71	5	50	-60	2.88	0.08
2007	4	10	16:34:25	69.73	-144.68	18	4.49	205	65	25	3.97	0.06
2007	4	28	5:20:30	69.65	-144.79	21	4.87	205	90	0	4.36	0.11
2007	5	8	15:46:49	45.39	-112.13	10	4.36	345	55	-85	3.7	0.08
2007	5	23	19:05:15	22.02	-96.27	11	5.6	190	75	-160	5.05	0.08
2007	5	25	13:40:18	25.96	-110.05	6	4.55	315	80	-160	3.99	0.06
2007	6	9	10:45:44	36.93	-104.79	4	3.35	195	50	-60	2.35	0.1
2007	6	10	18:06:06	66.27	-142.3	12	4.27	235	95	5	3.59	0.12
2007	6	11	1:03:46	37.5	-114.04	8	3.9	260	75	-5	2.79	0.06
2007	6	12	7:23:43	37.54	-118.88	14	4.55	40	75	-5	3.92	0.06
2007	6	14	21:57:57	45.13	-120.95	18	3.58	255	85	20	2.32	0.06
2007	6	25	2:32:26	41.13	-124.81	28	4.88	215	65	0	4.26	0.07
2007	8	6	5:59:45	37.81	-114.43	8	3.87	110	55	10	3.07	0.04
2007	9	1	18:32:02	41.64	-112.33	9	3.66	245	85	5	2.7	0.07
2007	9	8	7:15:40	33.67	-108.86	9	3.58	255	80	70	2.8	0.07

2007	9	24	6:20:54	45.1	-123.03	20	3.65	125	90	-45	2.82	0.1
2007	10	31	3:04:54	37.43	-121.77	9	5.48	235	85	-15	5.32	0.07
2007	11	3	15:35:32	66.32	-135.43	6	4.6	70	70	20	3.91	0.08
2007	11	3	19:55:05	66.05	-142.17	13	3.9	240	70	0	2.78	0.09
2007	11	5	21:48:00	39.36	-111.64	15	3.8	230	25	-65	2.98	0.07
2008	1	17	19:46:45	68.015	-136.149	18	4.92	250	70	15	4.49	0.09
2008	1	30	10:07:07	62.433	-137.052	12	4.29	85	40	60	3.79	0.1
2008	2	21	14:16:05	41.076	-114.771	11	5.91	30	40	-90	6	0.08
2008	2	21	23:57:52	41.053	-114.923	9	4.61	255	35	-40	4.15	0.09
2008	2	22	1:50:06	41.023	-114.932	11	3.86	230	55	-60	3.23	0.12
2008	2	22	23:27:46	41.043	-114.848	12	4.32	225	40	-85	3.75	0.09
2008	2	27	7:59:39	41.123	-114.676	11	4.12	90	85	10	3.7	0.07
2008	2	28	15:10:39	41.036	-114.897	10	3.98	250	40	-50	3.31	0.08

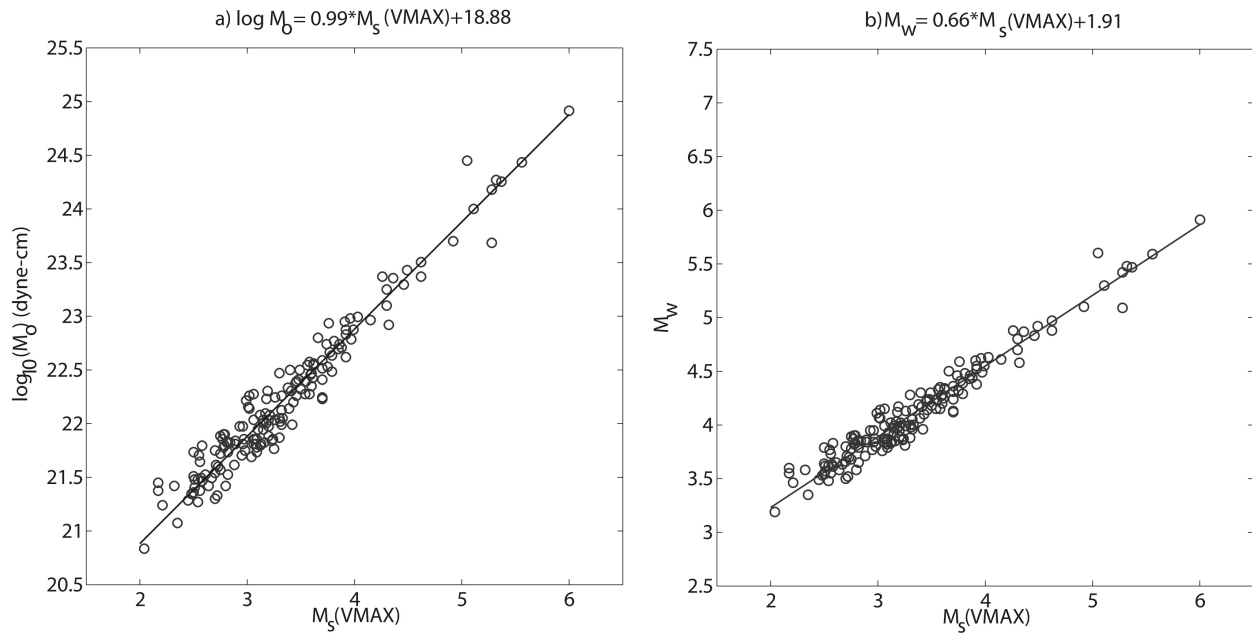


Figure 3. Orthogonal linear regressions of a) scalar moment ($\log M_0$) and b) moment magnitude (M_w) versus $M_s(VMAX)$. The moments were determined from broadband waveform modeling (Herrmann *et al.*, 2008). The solid lines are described by the linear equations at the top of each plot.

Table 2. Comparison of Different Regression Methods to Convert M_s (MVAX) to Moments

Estimating:	SR		ISR		GOR ($\eta=0.5$)		GOR ($\eta=2.0$)		OR ($\eta=1$)	
	Intercept	Slope	Intercept	Slope	Intercept	Slope	Intercept	Slope	Intercept	Slope
$\log M_o$ from M_s (VMAX)	18.9	0.97	18.8	1.03	18.9	1.01	18.9	0.99	18.9	0.99
M_w from M_s (VMAX)	1.95	0.65	1.82	0.69	1.9	0.66	1.93	0.65	1.91	0.66

Note that the standard regression (SR) methods is conceptually incorrect for our data in which the variance for M_s (MVAX) >0 . See Castellaro and Bormann (2007) for additional discussion.

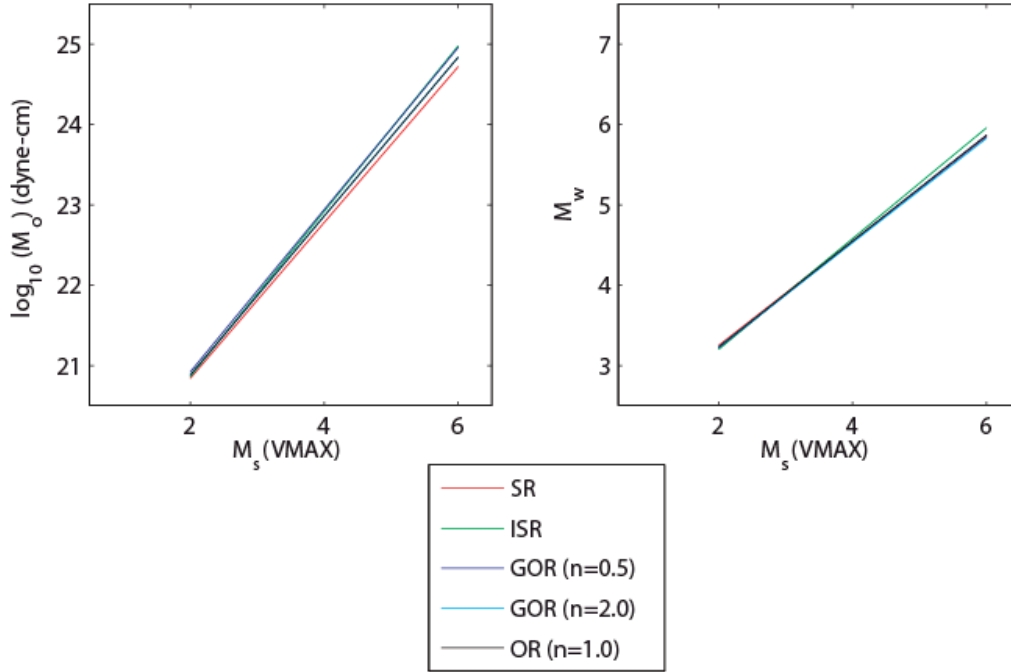


Figure 4. A comparison of the different linear regression methods described in Castellaro and Bormann (2007) applied to our M_s (VMAX) and moment data.

Scordilis (2006) used a global database to determine the relationship between M_s obtained from the NEIC and International Seismological Center (ISC) catalogs--both organizations use their preferred versions of the Vaněk et al. (1962) formula--and M_w from the Harvard CMT catalogs. Our resulting Equation 6 is similar to the results by Scordilis (2006) who found that:

$$\begin{aligned}
 M_w &= 2.07 + 0.67 M_s \quad (7) \\
 &\text{for } 3.0 < M_s < 6.1 \\
 M_w &= 0.08 + 0.99 M_s \\
 &\text{for } 6.2 < M_s < 8.2.
 \end{aligned}$$

As larger events in North America are analyzed using the current M_s (VMAX) techniques, we hope to derive a new relationship for events with $M_s > 6.0$.

Our results in Equation 6 agree less with Bormann *et al.* (2009), who found the relationship between M_s (BB)--a broadband application of the Vaněk et al. (1962) formula--and M_w was:

$$M_w = 1.68 + 0.74 M_s \quad (8)$$

for $4 < M_s < 6.8$.

To demonstrate the observed scatter, we calculated the residual M_w estimates as the network-averaged $M_w[M_s(\text{VMAX})]$ minus each estimate used to form the mean. The results for all events in our database are plotted as function of period and distance in Figure 5 with ± 1 standard deviation (σ) represented by the solid lines. For each period range, the $\pm 1\sigma$ lines are typically within ± 0.2 magnitude units (dashed lines) of the mean. There are no significant distance trends observable in the data at periods between 12 and 24 seconds. Distance trends at periods less than 10 seconds could be related to highly variable mid-to-upper crustal structure that is not effectively modeled by the attenuation operator in Equation 1. Efforts to regionalize the attenuation operator in Equation 1 have been attempted by Stevens et al. (2006) and Levshin et al., (2008). Also, distance trends at T=8 and 25 seconds could also be edge effects. We are experimenting with extending the $M_s(\text{VMAX})$ analysis to T=40 seconds to account for longer-period excitation for deeper events and have observed some reduction in the magnitude scatter at T=25 seconds.

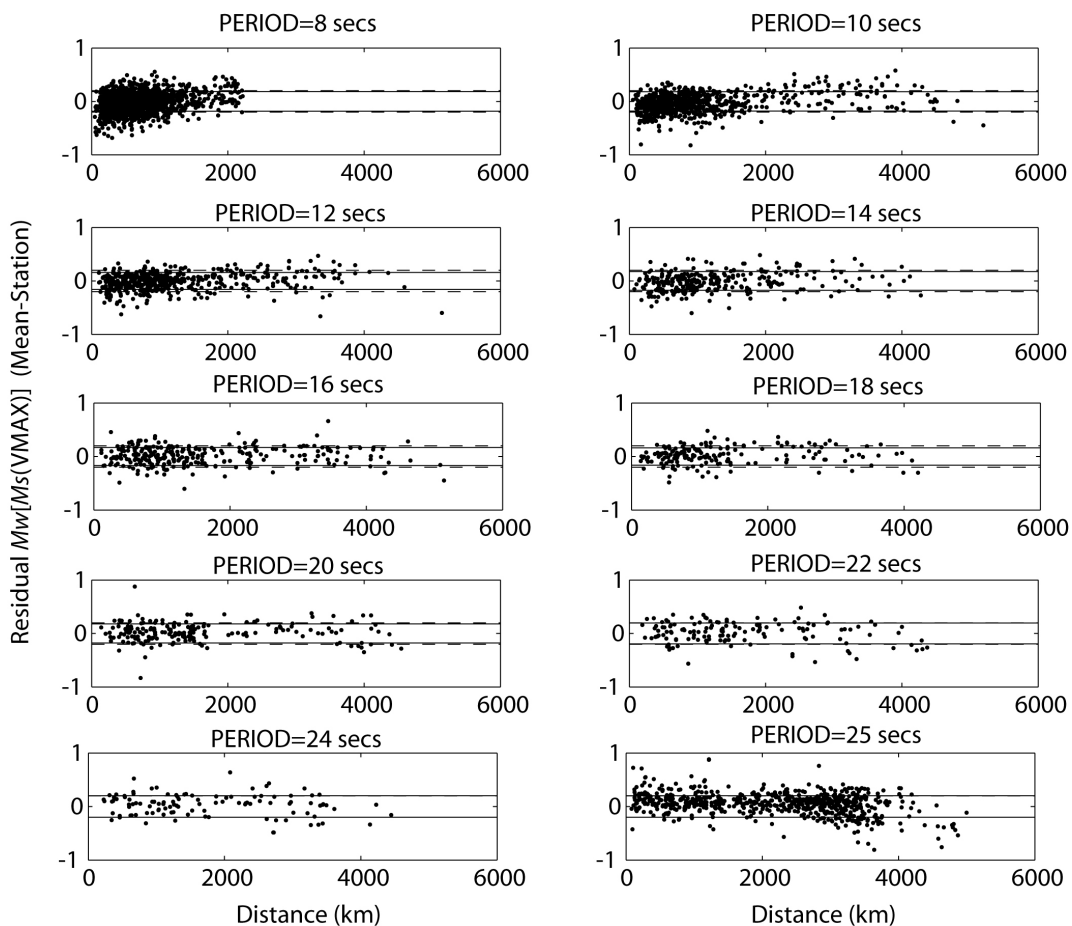


Figure 5. Scatter in $M_w[M_s(\text{VMAX})]$ estimates as function of evaluation period and distance. The dashed line represents ± 0.2 m.u. while ± 1 standard deviation (σ) is shown as the solid lines (for most periods, the two are very similar).

The residuals (Figure 6; Table 3) between $M_w[M_s(\text{VMAX})]$ and $M_w[\text{Waveform Modeling}]$ shows that there is little, if any, depth dependence on the predicted M_w 's for these crustal depth events. The results do indicate mechanism dependence for normal and strike-slip faulting sources. Each focal mechanism was classified as normal (NF) strike-slip (SS), thrust (TF), or oblique-slip variations of normal and thrust faults using the Zoback (1992) classification scheme. For normal faults, the $M_w[\text{Waveform Modeling}]$ is typically 0.04 m.u. smaller (Table 1) than the predicted $M_w[M_s(\text{VMAX})]$. A similar bias is suggested for thrust faulting but needs confirmation with more data. For strike-slip events, the $M_w[\text{Waveform Modeling}]$ is 0.07 m.u. larger than $M_w[M_s(\text{VMAX})]$. The reason for these differences results from our M_s estimates being based only on the Rayleigh waves. Strike-slip events release a large amount of long-period energy in the Love waves, which are not considered in our Rayleigh-wave technique. The opposite is true for normal faulting events, which produce more vertical (SV) motion resulting in over-predicting the M_w using $M_s(\text{VMAX})$. It could be possible to even further reduce these small biases by including Love waves or three-component analyses in the future.

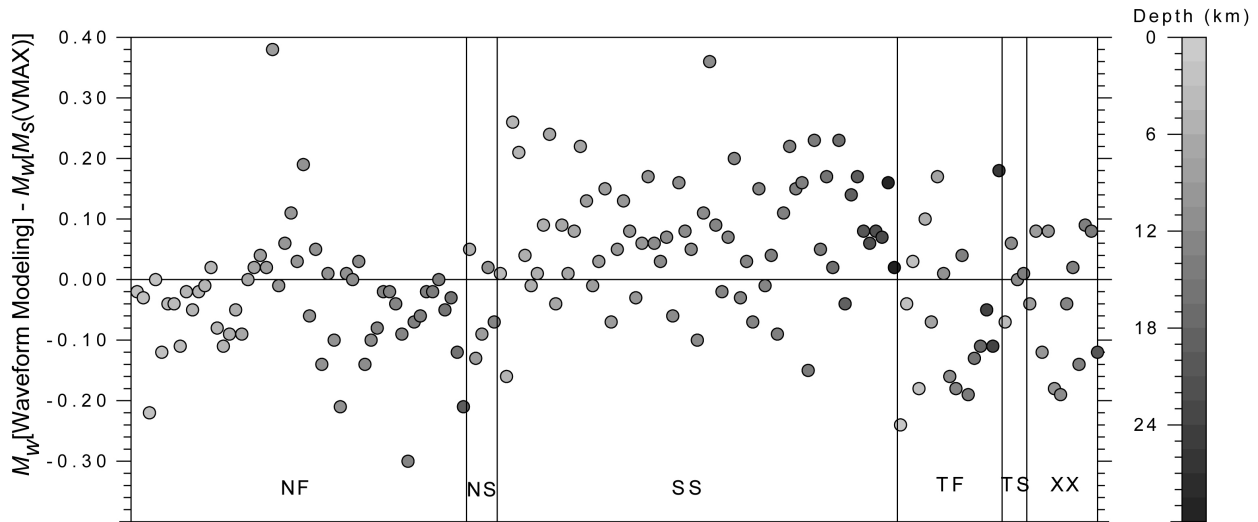


Figure 6. The dependence $M_w[M_s(\text{VMAX})]$ as a function of focal mechanism and depth. The mechanisms are based on the Zoback (1992) classification scheme and focal mechanisms of Herrmann et al. (2008). The faulting definitions include: SS=Strike-Slip, TF=Thrust Fault, NF=Normal Fault, TS=Thrust with Strike-Slip component, NS=Normal with Strike-Slip component and XX=Unknown. The residuals between $M_w[\text{Waveform Modeling}]$ and $M_w[M_s(\text{VMAX})]$ have a definable faulting mechanism effect, especially when strike-slip events are compared to those with other mechanisms.

Table 3. Statistical Analysis of M_w [Waveform Modeling] - M_w [M_s (VMAX)]

Mechanism	Mean	SD	Standard Error of the Mean	Observations
SS	0.07	0.10	0.01	65
TF	-0.05	0.13	0.03	17
NF	-0.04	0.10	0.01	54
TS	-0.00	0.05	0.03	4
NS	-0.04	0.08	0.03	5
XX	-0.04	0.11	0.03	12

VALIDATION TESTING

We tested the M_s (VMAX): M_w relationship (Equation 6) on a validation dataset consisting of 34 North American events with $3 < M_w < 6$ that occurred during the first 10 months of 2009 (Table 4). The focal mechanisms are compiled at http://www.eas.slu.edu/Earthquake_Center/MECH.NA/ (last accessed March, 2010) and include a variety of different faulting solutions with depths ranging from 1 to 69 km. Data were again downloaded from IRIS and the USGS, converted to displacement in nanometers, and M_s (VMAX) was estimated and converted to M_w using Equation 6.

We averaged the M_w [M_s (VMAX)] as a function of time after the event. Figure 7 shows three examples of this averaging technique. The mean M_w [M_s (VMAX)] for each station is shown as a circle with ± 1 standard deviation (σ) presented as the vertical error bars—except for the first station that recorded the event for which σ cannot be estimated. Abrupt increases in the standard deviation are related to inclusion of an anomalous or outlier measurement, possibly caused by incorrect instrument responses, measurement errors, or radiation pattern effects such as propagation nulls. The dashed horizontal line is the observed M_w [Waveform Modeling]. We arbitrarily chose a time of 5 minutes after origin to examine the performance of this method. This corresponds to Rayleigh-wave propagation distances between 600 km and 1200 km based on our processing windows of 2 km/sec to 4 km/sec, respectively. Preliminary locations, which are needed for magnitude estimation, are often available by 5 minutes after North American event origins. At 5 minutes after the origin of the event, all three of these events would have an M_w [M_s (VMAX)] within $\pm 2\sigma$ of the observed moment magnitude.

The comparison of the M_w [M_s (VMAX)] (at 5 minutes after the origin) to the observed M_w [Waveform Modeling] for all 34 events is shown in Figure 8. With the exception of three events, all of the M_w [M_s (VMAX)] were within 0.2 m.u. of the observed M_w . Of these three outlier events, two were at depths greater than 50 km and were deeper than the events used to develop Equation 6. Table 4 provides the final estimates as a function of time, and we note < 0.03 m.u. average difference between the final M_w [M_s (VMAX)] and the estimates using surface waves observed within 5 minutes after the event origin.

Table 4. Origin Information for the Validation Test

Year	Month	Day	UTC	Latitude	Longitude	Depth (km)	M_w	Strike	Dip	Rake	M_s (VMAX) @ 5 Minutes	#Obs	M_w (PRE) @ 5 Minutes	STD	M_w (PRE) FINAL
2009	1	2	14:17:13	58.53	-152.25	62	5.18	235	80	35	4.39	4	4.81	0.04	4.78
2009	1	16	4:15:36	43.23	-110.86	8	4.02	190	35	-85	3.21	11	4.03	0.08	4.02
2009	1	17	13:56:43	63.61	-150.86	9	4.22	20	60	30	3.42	9	4.17	0.13	4.11
2009	1	30	13:25:04	47.80	-122.54	55	4.52	125	75	-10	3.22	15	4.04	0.07	4.02
2009	2	24	16:20:23	62.93	-143.68	13	3.96	270	50	15	3.06	9	3.93	0.11	3.90
2009	2	26	9:52:47	42.54	-123.89	43	4.19	325	70	-75	3.30	5	4.09	0.07	4.07
2009	3	21	8:47:50	43.33	-110.73	6	3.35	50	75	-15	2.24	9	3.39	0.04	3.40
2009	3	21	19:17:54	62.06	-79.65	1	3.78	95	35	90	3.03	8	3.91	0.17	4.01
2009	3	24	11:55:43	33.32	-115.74	3	4.66	55	70	-15	4.43	27	4.83	0.05	4.80
2009	3	27	2:58:39	61.01	-138.41	13	4.94	285	70	75	4.45	9	4.85	0.07	4.86
2009	3	28	14:11:21	60.93	-138.33	13	4.08	65	25	50	3.19	11	4.02	0.13	4.01
2009	4	21	10:25:44	33.01	-87.15	6	3.35	275	85	-10	2.17	2	3.34	0.1	3.34
2009	4	30	4:54:57	58.98	-151.30	45	4.90	20	25	-75	4.32	14	4.76	0.08	4.75
2009	5	1	1:33:58	36.85	-104.78	8	3.13	185	85	20	1.98	2	3.22	0.09	3.22
2009	5	17	6:45:18	42.54	-108.12	17	3.70	310	30	-35	2.93	30	3.84	0.09	3.83
2009	5	28	13:57:30	66.32	-135.16	12	3.87	5	35	55	2.99	5	3.88	0.04	3.87
2009	5	29	18:16:01	48.52	-112.34	2	3.16	160	35	95	2.31	22	3.43	0.07	3.43
2009	6	7	23:24:39	58.97	-136.72	15	4.75	155	50	45	4.45	14	4.85	0.08	4.85
2009	6	22	19:28:05	61.94	-150.52	63	5.34	25	55	-40	4.92	15	5.16	0.08	5.13
2009	6	23	14:27:56	61.93	-150.68	55	3.95	40	45	-10	3.11	3	3.96	0.13	4.02
2009	6	30	18:52:10	66.00	-151.84	15	3.81	215	65	-30	2.91	11	3.83	0.17	3.82
2009	7	3	11:00:19	25.47	-109.64	7	5.79	230	60	10	5.80	15	5.74	0.07	5.75
2009	7	7	19:11:45	75.28	-72.20	13	6.00	150	45	55	5.96	4	5.84	0.04	5.93
2009	7	21	14:20:55	49.81	-65.71	15	3.54	0	60	75	2.51	6	3.57	0.07	3.60
2009	7	29	10:00:36	36.82	-104.80	4	4.04	15	65	-65	3.24	173	4.05	0.1	4.08
2009	8	17	0:22:12	38.47	-102.73	10	3.85	70	50	-80	3.12	28	3.97	0.16	4.00
2009	8	18	2:50:16	40.62	-107.64	18	3.69	145	55	-20	2.74	30	3.72	0.08	3.72
2009	8	19	18:19:27	61.21	-150.81	69	4.92	85	25	25	4.34	11	4.77	0.17	4.76
2009	8	28	21:42:19	63.48	-148.33	12	3.90	180	35	35	3.05	10	3.92	0.09	3.94
2009	9	14	18:27:23	36.55	-106.47	12	3.45	245	60	-20	2.41	6	3.50	0.05	3.51
2009	9	21	10:41:26	60.92	-147.12	27	4.30	195	70	-70	3.72	15	4.37	0.07	4.35
2009	9	23	13:03:14	34.48	-107.90	5	3.44	5	60	-65	2.42	14	3.51	0.06	3.50
2009	10	9	22:13:54	35.96	-114.55	9	3.46	105	85	20	2.51	4	3.57	0.07	3.57
2009	10	13	13:03:33	63.46	-145.05	13	3.84	260	55	60	3.07	10	3.94	0.12	3.98

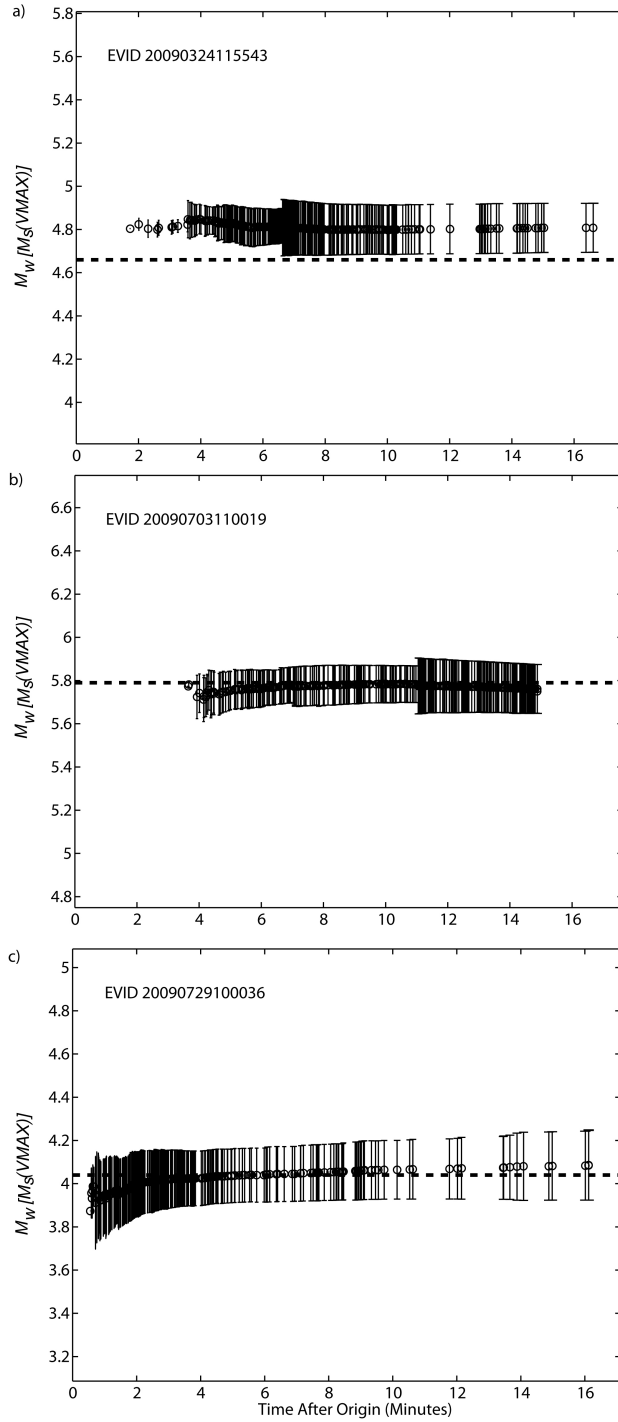


Figure 7. $M_w[M_s(\text{VMAX})]$ as a function of time after event origin for three events in our validation dataset. The events occurred on a) 24 March 2009 at 11:55:43 b) 03 July 2009 at 11:00:19 and c) 29 July 2009 at 10:00:36. The mean for each station is shown as a circle with ± 1 standard deviation (σ) presented as the vertical error bars. The dashed horizontal line is the observed M_w based on waveform modeling.

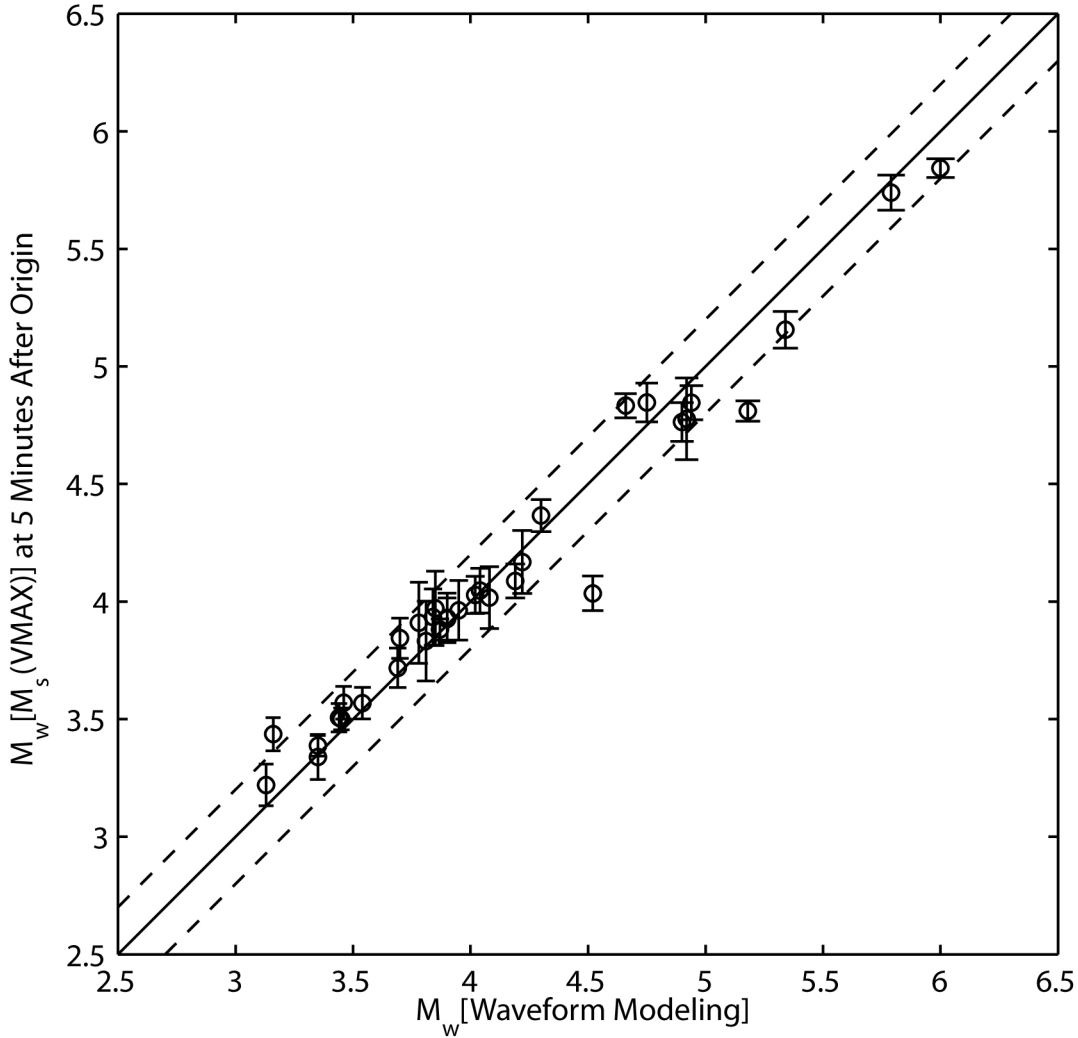


Figure 8. $M_w[M_s(\text{VMAX})]$ at five (5) minutes after event origin versus $M_w[\text{Waveform Modeling}]$. The solid line is the 1:1 relation with ± 0.2 m.u. plotted as dashed lines. Vertical error bars represent $\pm 1 \sigma$.

CONCLUSIONS

A rapid and robust estimate of seismic moment can be achieved for crustal depth North American earthquakes with $2 < M_s < 6$ using near-regional surface wave magnitudes and the equation $M_w = 1.91 + 0.66 M_s$. Small changes to this equation can arise from different assumptions used in the linear regression analysis; however, the resulting estimate of M_w will vary by less than 0.1 m.u. from our preferred equation. The variance of this method of estimating moments from surface wave magnitudes will be slightly higher than waveform modeling techniques due to focal mechanism-produced biases that are not accounted for when analyzing only Rayleigh-waves for surface wave magnitudes. However, because $M_s(\text{VMAX})$ is easy to automate in an operational setting and accounts for some of the complexities of near-

regional surface wave propagation, the M_s -predicted M_w can be estimated as soon as the first surface wave arrives from an event and an initial epicentral location has been formed. A validation tests suggests that given a number of stations situated at local and near-regional distances from the epicenter, the estimated M_w after the final surface waves arrive will not differ significantly from the M_w estimated within the first five minutes. The M_w estimation by the conversion of surface wave magnitudes could provide the USGS PAGER system with an initial value that would then be updated as teleseismic body wave modeling and CMT results become available.

DATA AND RESOURCES

We thank the USGS, IRIS, and NRCAN for access to their invaluable data archives. Thanks also to the many seismic network operators whose dedication make this effort possible: University of Alaska, University of Washington, Oregon State University, University of Utah, Montana Bureau of Mines, UC Berkeley, Caltech, UC San Diego, Saint Louis University, University of Memphis, Lamont Doherty Earth Observatory, Boston College, the IRIS stations and the Transportable Array of EarthScope.

ACKNOWLEDGEMENTS

We thank Dr. David Russell for his assistance with this collaboration and research. We also thank Drs. David Harkrider, Anastasia Stroujkova, Robert Shumway, and Michael Pasyanos for their input at various stages of the project. We greatly appreciate a review by Jim Dewey who helped clear up several misconceptions we had regarding historical M_s research. We also appreciate additional reviews of the manuscript by Morgan Moschetti and other USGS researchers. We thank Silvia Castellaro for reviewing the document and greatly improving the linear regression analyses. We thank Mr. Jim Lewkowicz for his continued support and thoughtfulness. Part of this research was funded under the auspices of the Department of Energy's National Nuclear Security Administration under Contract No. DE-AC52-04NA25547. Additional funding was provided through the National Earthquake Hazards Program, Award No. G09AP00078.

REFERENCES

- Bonner, J. L., D. Russell, D. Harkrider, D. Reiter, and R. Herrmann, (2006). Development of a Time-Domain, Variable-Period Surface Wave Magnitude Measurement Procedure for Application at Regional and Teleseismic Distances, Part II: Application and $M_s - m_b$ Performance. *Bull. Seism. Soc. Am.* **96**, 678–696.
- Bonner, J., R. B. Herrmann, and H. Benz (2008). Rapid estimates of seismic moment using variable-period surface-wave magnitudes. Abstract. *Seism. Res. Letts.* **79**, 349.
- Bormann, P., R. Liu, Z. Xu, K. Ren, L. Zhang, and S. Wendt (2009). First application of the new IASPEI teleseismic magnitude standards to data of the China National Seismograph Network. *Bull. Seism. Soc. Am.*, **99**, 1868-1891.
- Castellaro, S. and P. Bormann (2007). Performance of different regression procedures on the magnitude conversion problem. *Bull. Seism. Soc. Am.* **97**, 1167-1175.

- Earle, P., D. J. Wald, K. A. Porter, J.S. Jaiswal, and T. I. Allen (2008). An overview of the USGS PAGER (Prompt Assessment of Global Earthquakes for Response) system. *Seism. Res. Letts.* **79**, 313.
- Ekström, G. and A. Dziewonski (1988). Evidence for bias in estimations of earthquake size. *Nature*, 332. 319-323.
- Gutenberg, B., (1945). Amplitudes of surface waves and the magnitudes of shallow earthquakes. *Bull. Seism. Soc. Am.* **35**, 3.
- Hanks, T. and H. Kanamori (1979). A moment magnitude scale, *J. Geophys. Res.* **84**, 2348-2350.
- Herak, M. and D. Herak (1993). Distance dependence of M_s and calibrating function for 20 second Rayleigh waves, *Bull. Seism. Soc. Am.*, **83**, 1681.
- Herrmann, R.B., H. Benz, and C. Ammon (2008). Systematic moment tensor estimation for North America earthquakes. Abstract. *Seism. Res. Letts.* **79**, 349.
- Herrmann, R. B. And L. Malagnini (2009). Fault dynamics of the April 6, 2009 L'Aquila Italy earthquake sequence (draft).
- Levshin, A., M. Barmin, X. Yang, and M. Ritzwoller (2008). Toward a Rayleigh wave attenuation model for Asia and surrounding regions. *Proceedings of the 30th Monitoring Research Review: Ground-Based Nuclear Monitoring Technologies*. LA-UR-08-05261. Volume 1. Pp. 108-117.
- Marshall, P.D. and P.W. Basham, (1972). Discrimination between earthquakes and underground explosions employing an improved M_s scale. *Geophys. J. R. Astr. Soc.* **29**, 431–458.
- Rezapour, M., and R.G. Pearce, (1998). Bias in surface-wave magnitude M_s due to inadequate distance correction. *Bull. Seism. Soc. Am.* **88**, 43–61.
- Russell, D. R. (2006). Development of a time-domain, variable-period surface wave magnitude measurement procedure for application at regional and teleseismic distances, part I: theory, *Bull. Seism. Soc. Am.* **96**, 665–677.
- von Seggern, D., (1977). Amplitude distance relation for 20-Second Rayleigh waves. *Bull. Seism. Soc. Am.* **67**, 405-411.
- Scordilis, E.M. (2006). Empirical global relations converting M_s and m_b to moment magnitude. *J. Seism.* **10**, 225-236.
- Stevens, J. L. and K.L. McLaughlin, (2001). Optimization of surface wave identification and measurement, in *Monitoring the Comprehensive Nuclear Test Ban Treaty: Surface Waves*, eds. Levshin, A. and M.H. Ritzwoller, *Pure Appl. Geophys.*, **158**, 1547-1582.
- Stevens, J., J. Given, G. Baker, and H. Xu. (2006). Development of surface wave dispersion and attenuation maps and improved methods for measuring surface waves. In *Proceedings of the 28th Seismic Research Review: Ground-Based Nuclear Explosion Monitoring Technologies*, LA-UR-06-5471, Vol. 1, pp. 273-281.
- Vaněk, J., A. Zatopek, V. Karnik, Y.V. Riznichenko, E.F. Saverensky, S.L. Solov'ev, and N.V. Shebalin, (1962). Standardization of magnitude scales. *Bull. (Izvest.) Acad. Sci. U.S.S.R., Geophys. Ser.*, **2**, 108.
- Zoback M.L. (1992). First- and second-order patterns of stress in the lithosphere: the world stress map project, *J. Geophys. Res.*, **97**, 11703-11728.

BIBLIOGRAPHY

J. Bonner, R. Herrmann, and H. Benz (2010). Variable-Period Surface-Wave Magnitudes: A Rapid and Robust Estimator of Seismic Moments. *Bulletin of the Seismological Society of America*, October 1, 2010; 100(5A): 2301 - 2309.

APPENDIX: APPLICATION IN CENTRAL ITALY

We have also developed a relationship between moment magnitude (M_w) and surface wave magnitude (M_s) for earthquakes occurring in Italy, with a primary focus on the L'Aquila earthquake (6 April 2009 M_w 6.1) and its aftershocks. We used the Russell (2006; Bonner et al., 2006) variable-period surface wave magnitude formula, henceforth called M_s (VX), to estimate the M_s for 125 Italian earthquakes with $2.8 < M_w < 6.1$ at distances ranging from 50 to 414 km. We applied the technique to Rayleigh and Love waves, resulting in 1449 and 1142 magnitude estimates, respectively. The network-averaged magnitudes show that most of the events (80%) had a Love-wave M_s that was larger (average 0.2 m.u.) than the Rayleigh-wave estimate. The larger Love-wave magnitudes are somewhat unexpected for the normal fault focal mechanisms (Herrmann and Malagnini, 2009) of the L'Aquila sequence. We observe larger interstation standard deviation for the Love-wave magnitudes (0.2 m.u.) than for Rayleigh waves (0.17 m.u.). Residual M_s (VX) estimates (e.g., station minus network average) show no significant distance dependence on the magnitudes; however, there is a clear azimuthal effect on the Rayleigh-wave station residuals. The largest residuals are observed at azimuths parallel and perpendicular to the predominant strike ($\sim 330^\circ$) of the events. An azimuthal effect on the Love waves is less obvious. The interstation standard deviations can be reduced by $\sim 15\%$ by correcting for azimuthal effects. M_w estimated from broadband waveform modeling were regressed against M_s (VX). M_w can be estimated from M_s (VX) and Rayleigh waves using the relationship: $M_w = 1.78 + 0.68 * M_s$ (VX) for $2 < M_s < 6$, while for Love waves, the relationship is $M_w = 1.64 + 0.69 * M_s$ (VX) (Figure A-1).

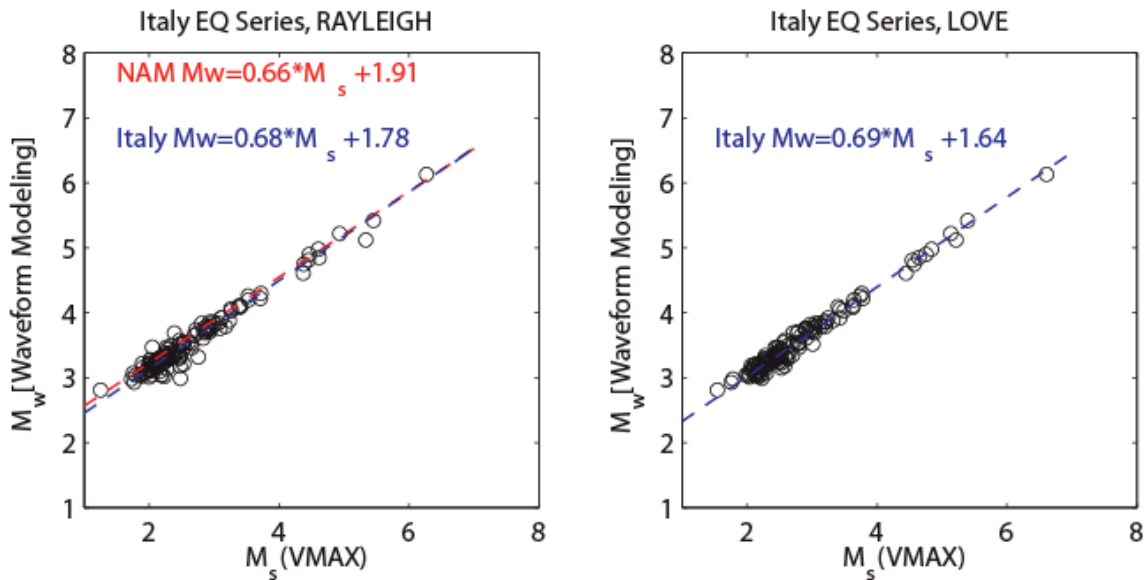


Figure A- 1. Orthogonal linear regressions of moment magnitude (M_w) versus M_s (VMAX) for Rayleigh (left) and Love (right) waves from central Italian earthquakes. The moments were determined from broadband waveform modeling (Herrmann and Malagnini, 2009). The solid lines are described by the linear equations at the top of each plot.